PQ THEORY-BASED MODELLING AND SIMULATION OF A SHUNT ACTIVE POWER FILTER FOR IMPROVING POWER QUALITY

Sabin Kasula*

Department of Electrical Engineering, Khwopa College of Engineering, Bhaktapur, Nepal

Abstract

Over the past decades, there has been a significant rise in the use of nonlinear loads which draw harmonic, distorted current, and voltage at the point of connection with the utility grid. This distorted voltage and current affect the power system and also the end consumers. So, meeting the power quality criteria of the utility grid has become essential in the modern power system. In this paper, a comprehensive, organised methodology for designing a shunt active power filter (SAPF) is presented, highlighting its role as an efficient tool for power quality enhancement, providing reactive power compensation, and mitigation of distortion problems. The PQ theory is implemented to determine the reference currents, and hysteresis current control is utilised to generate the gate pulses that manage the switching of the voltage source inverter (VSI). The complete SAPF is validated through simulation in MATLAB/Simulink for non-linear balanced and unbalanced loads. The simulation response shows that the presented SAPF filter effectively mitigates harmonic distortion, which is below the standard thresholds of the Institute of Electrical and Electronics Engineers (IEEE). For non-linear balanced load conditions, the Total Harmonic Distortion (THD) is suppressed to 0.29%, while for non-linear unbalanced load conditions, the THD decreases to 1.81%.

Keywords: Shunt Active Power Filter (SAPF), Instantaneous Power Theory Control Strategies, Harmonic Compensation, Hysteresis Current Control.

1. Introduction

The increasing application of nonlinear loads, primarily driven by power electronic devices, has introduced power quality (PQ) issues in electric power distribution networks Sahu et al. (2020). This has led to a continuous rise in harmonic emissions, current imbalance, and high reactive power consumption Kmail (2012). The presence of harmonic currents not only leads to voltage harmonics but also introduces various disturbances in the power grid. So the concern related to harmonics has increased due to their negative consequences, such as resonance in series and parallel circuits, additional power losses in feeders, transformers, malfunctioning of protection systems, inaccuracies in measurement devices, and other loads that are highly sensitive to harmonics Adel et al. (2011) and F II (1993). The IEEE Standards Association (IEEE-SA) established harmonic current limits for power systems in IEEE Std 519-1992 Kmail (2012), which were later revised in IEEE Std 519-2014. According to this standard, the THD should remain below 5% Imam et al. (2020). Consequently, power filters are used to maintain this requirement.

The previous studies show that SAPFs are effective and widely adopted technologies for mitigating the propagation of harmonic distortion. Traditionally, in power distribution networks, harmonic currents are usually reduced by using both shunt and series passive filters. Moreover, the passive filter is associated wsith several limitations, including an inability to compensate for random frequency variations, reduced filtering effectiveness due to parameter changes, tuning difficulties, and the risk of parallel resonance. To overcome classic filters' limitation, active power filters (APFs) have been developed, which cancel current harmonics by injecting equal but opposite distortions, thereby enhancing overall power quality Adel et al. (2011)

*Corresponding author: Sabin Kasula
Department of Electrical Engineering, Khwopa College of Engineering, Bhaktapur, Nepal
Email: sabinkasula32@gmail.com
(Received: October 28, 2025, Accepted: May 13, 2026)
https://doi.org/10.3126/jsce.v13i2.96575

and Imam et al. (2020).

The effectiveness of a SAPF in mitigating harmonics relies largely on the method used for the detection of current harmonics and reactive power, along with the applied compensation control algorithm Adam et al. (2012). Among the various reference current control techniques, the PQ Theory is the most commonly adopted. In 1983, the overall representation form of this idea was originally introduced by Akagi et al.Akagi et al. (1983). Gary W. et al. Chang and Shee (2004) proposed a technique to reduce harmonic currents in a three-phase, four-wire system under unbalanced voltage conditions. Kanjiya Kanjiya et al. (2012) conducted real-time testing of a SAPF driven by a single-step, non-iterative optimized control algorithm. The findings confirmed that the system harmonics current is reduced under both transient as well as steady state load scenarios.

This paper presents a detailed procedure for a MATLAB/Simulink model of a SAPF that utilizes the IRPT concept to extract reference currents. The harmonic current regulation method is implemented on a three-phase, four-wire supply, based on both unbalanced and balanced nonlinear loads. The effectiveness of the system is determined by measuring the source current's THD and its power factor correction performance.

The remainder of the paper is structured as follows. Section 2 details the proposed control methodologies. Section 3 details the results and discussion, Section 4 provides the conclusion of the paper, and Section 5 highlights limitations along with directions for future research.

2. Implementation Details

2.1. Shunt Active Power Filter: Topology and Operational Principles

Figure 1 illustrates the general setup of a typical VSI -based SAPF, considered as the primary case in this paper. Normally, the SAPF is installed at the Point of Common Coupling (PCC) of a harmonic-affected power system.

The primary role of the SAPF is to improve power quality in electrical distribution systems by eliminating current harmonics produced by nonlinear loads, compensating reactive power, and balancing load currents. The system consists of two main sections, namely the power section and the control section. The power section consists of a DC-link capacitor or battery that generates the compensating current and a PWM-driven VSI. In order to determine the instantaneous reference compensating current, the control circuit continuously monitors changes in harmonic currents and directs the power circuit to accurately generate the necessary harmonic components. The control circuit continuously observes harmonic current variations, computes the compensation reference current, and commands the power section to generate the corresponding harmonics with precision Hoon et al. (2019) and Imam et al. (2020).

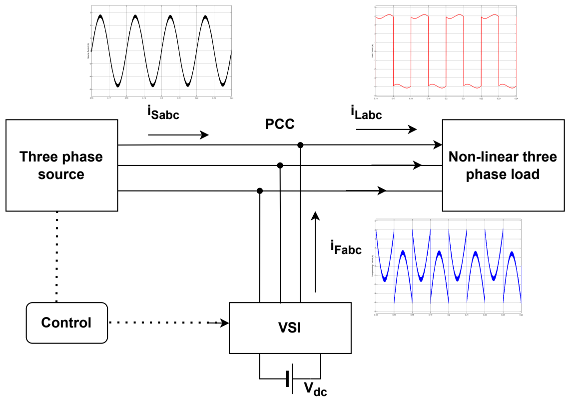

Figure 1: System configuration of three-phase VSI-based SAPF.

At the PCC, applying KCL gives the current in the system affected by harmonics before SAPF installation as Hoon et al. (2019):

$$i_S = i_L = i_{1L} + i_H \tag{1}$$

Here, i_S represents the source current, while i_L denotes the load current, which consists of the fundamental component i_{1L} and the harmonic component i_H generated by nonlinear loads. The primary objective of the SAPF is to eliminate these harmonic currents. Once the SAPF is installed at the PCC, it injects a compensating current i_f into the system, which is the same in magnitude, having a phase opposite to i_H, thereby canceling the harmonics. Accordingly, by applying KCL, Equation (1) can be rewritten as shown in Equation (2) Hoon et al. (2019):

$$i_S = i_L = i_{1L} + i_H - i_f \tag{2}$$

Since the SAPF provides a compensating current i_f equal in magnitude and having a phase shift of 180 degrees relative to the harmonic current i_H, the source current is reduced to the fundamental component as shown in Equation (3) Hoon et al. (2019):

$$i_S = i_{1L} + i_{dc} \tag{3}$$

To better illustrate the operation of the SAPF, Figure 2 shows an example waveform including the source voltage v_s, load current i_L, resulting source current i_s, and compensating current i_f. In this example, a balanced sinusoidal source voltage is considered using the nonlinear load that includes a three-phase uncontrolled bridge rectifier with an RL load.

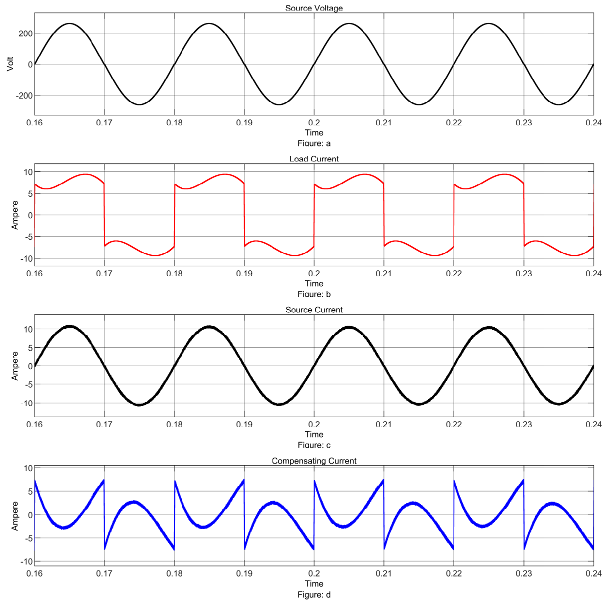

Figure 2: Voltage and current profile indicating the power system behaviour with SAPF installed. (a) depicts the source voltage v_s; (b) represents the load current i_L; (c) represents the source current i_s; and (d) represents the compensating current i_f.

2.2. Instantaneous Active and Reactive Power Control Strategy

In this paper, the time-domain formulation of PQ Theory is presented, and a corresponding simulation model is developed in MATLAB/Simulink. Figure 3 illustrates the block diagram for the extraction of reference current using the PQ concept. The principle of this theory relies on transforming the three-phase stationary reference frame (a-b-c) into the 0-α-β reference frame using the Clarke transformation. Through this transformation, the source voltages and currents are expressed in terms of their 0-α-β components, as described by the following equations Imam et al. (2020). In Equation (4) Akagi et al. (1983) the three-phases voltage (a-b-c) are transform into 0-α-β reference frame wheras Equation (5) Akagi et al. (1983) represent the three-phases current transformation to 0-α-β reference frame.

$$\begin{bmatrix} v_0 \\ v_\alpha \\ v_\beta \end{bmatrix} = \sqrt{\frac{2}{3}} \begin{bmatrix} \frac{1}{\sqrt{2}} & \frac{1}{\sqrt{2}} & \frac{1}{\sqrt{2}} \\ 1 & -\frac{1}{2} & -\frac{1}{2} \\ 0 & \frac{\sqrt{3}}{2} & -\frac{\sqrt{3}}{2} \end{bmatrix} \begin{bmatrix} v_a \\ v_b \\ v_c \end{bmatrix} \tag{4}$$

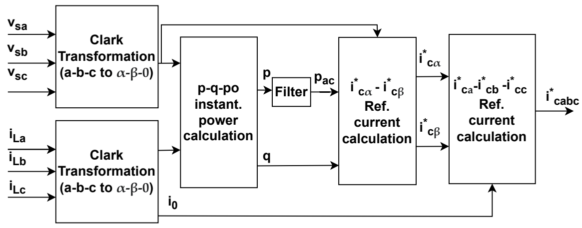

Figure 3: Reference current extraction with PQ Theory method.

$$\begin{bmatrix} i_0 \\ i_\alpha \\ i_\beta \end{bmatrix} = \sqrt{\frac{2}{3}} \begin{bmatrix} \frac{1}{\sqrt{2}} & \frac{1}{\sqrt{2}} & \frac{1}{\sqrt{2}} \\ 1 & -\frac{1}{2} & -\frac{1}{2} \\ 0 & \frac{\sqrt{3}}{2} & -\frac{\sqrt{3}}{2} \end{bmatrix} \begin{bmatrix} i_a \\ i_b \\ i_c \end{bmatrix} \tag{5}$$

Here, v_a, v_b, and v_c are the three-phase voltages and i_a, i_b, and i_c are the corresponding three-phase currents in the a–b–c frame. The transformed voltage and current components v_0, v_α, v_β and i_0, i_α, i_β are defined in 0–α–β reference frame.

In this study, a four-wire three-phase distribution system is analyzed. According to the IRPT Theory, the active, reactive, and zero-sequence powers are defined as in Equation (6) Mikkili and Panda (2011a).

$$\begin{bmatrix} p_0 \\ p \\ q \end{bmatrix} = \begin{bmatrix} v_0 & 0 & 0 \\ 0 & v_\alpha & v_\beta \\ 0 & v_\beta & -v_\alpha \end{bmatrix} \begin{bmatrix} i_0 \\ i_\alpha \\ i_\beta \end{bmatrix} \tag{6}$$

Here, Equation (7) Akagi et al. (1983) represents the instantaneous active power exchanged between the source and the load in the α-β plane. Equation (8) Akagi et al. (1983) presents the instantaneous reactive power, which doesn't contribute to net energy transfer. It is associated with the energy oscillation between the source and reactive elements, whereas Equation (9) Akagi et al. (1983) shows the zero sequence power due to the unbalanced loads or neutral current.

$$p = v_\alpha i_\alpha + v_\beta i_\beta, \tag{7}$$
$$q = v_\alpha i_\beta - v_\beta i_\alpha, \tag{8}$$
$$p_0 = v_0 i_0 \tag{9}$$

In nonlinear loads, the instantaneous active and reactive power are separated into DC and AC components, as expressed in Equations (10) and (11) Imam et al. (2020). The DC part of the real power represents the fundamental component delivered from the source to the load, with the AC part representing the oscillatory energy exchange. The average (DC) component, which is the only portion supplied by the three-phase AC source, is obtained using a high-order low-pass filter. Similarly, the reactive power consists of fundamental and harmonic parts, responsible for energy circulation among load phases Afonso et al. (2000).

$$P = \bar{p} + \tilde{p} \tag{10}$$

$$Q = \bar{q} + \tilde{q} \tag{11}$$

For harmonic reference current generation, the AC component of the real power $(\tilde{p})$ and the total oscillating power (Q) are utilized. The AC part of real power is obtained as given in Equation (12). Using this, the compensation reference currents are first computed in the α - β frame, as expressed in Equation (13), and then transformed quantities are finally mapped back to the a–b–c frame using inverse Clark transformation as given in Equation (14) Imam et al. (2020).

$$\tilde{p} = P - \bar{p} \tag{12}$$

$$\begin{bmatrix} i^*_{c\alpha} \\ i^*_{c\beta} \end{bmatrix} = \frac{1}{v_\alpha^2 + v_\beta^2} \begin{bmatrix} v_\alpha & -v_\beta \\ v_\beta & v_\alpha \end{bmatrix} \begin{bmatrix} \tilde{p} \\ Q \end{bmatrix} \tag{13}$$

$$\begin{bmatrix} i^*_{ca} \\ i^*_{cb} \\ i^*_{cc} \end{bmatrix} = \sqrt{\frac{2}{3}} \begin{bmatrix} 1 & 1 & 0 \\ -\frac{1}{2} & -\frac{1}{2} & \frac{\sqrt{3}}{2} \\ -\frac{1}{2} & -\frac{1}{2} & -\frac{\sqrt{3}}{2} \end{bmatrix} \begin{bmatrix} i_0 \\ i^*_{c\alpha} \\ i^*_{c\beta} \end{bmatrix} \tag{14}$$

2.3. Current Control Techniques

Current controllers play an essential role in SAPF operation, as they adjust the compensating currents injected at the PCC to eliminate harmonics and reactive power. There are different current control methods, such as hysterisis, PI (Proportional-Integral), PR (Proportional-Resonant), deadbeat, sliding mode, predictive, and fuzzy logic control, each offering distinct advantages and drawbacks.

In comparison, hysteresis control is easy to implement and robust, offering rapid transient performance; however, its variable switching frequency leads to increased current ripple and higher switching losses Kanagavel and Indragandhi (2019). PI current control works at a fixed switching frequency and is easy to set up. However, it exhibits limited dynamic response and requires an accurate model of the system, even though low harmonic distortion can be achieved with proper tuning Daniyal et al. (2011). Model predictive control (MPC) and dead-beat methods offer extremely quick dynamic response and low harmonic distortion; however, they are less reliable and require a lot of computational power Kanagavel and Indragandhi (2019). Intelligent controllers, such as ANN or fuzzy logic, can efficiently manage system nonlinearities and achieve a fixed switching frequency operation; however, they require a detailed understanding of the SAPF system's behaviour and operation, along with substantial training Kanagavel and Indragandhi (2019).

The hysteresis control approach is chosen for its fast dynamic behavior, effective current limiting, and simple design Iqbal et al. (2021) and Chavali et al. (2024).The estimated reference currents $i^*_{ca}, i^*_{cb}, i^*_{cc}$ are evaluated with the measured compensating currents i_{fa}, i_{fb}, i_{fc} using a hysteresis band controller. The resulting error signal is employed to produce the switching gate pulses for the VSI inverter. In this setup, the compensating currents i_{fabc} are made to track the reference currents i^*_{cabc} within a specified hysteresis band Mikkili and Panda (2011b). Figure 4 shows the Hysterisis current controller with PWM pulse generation.

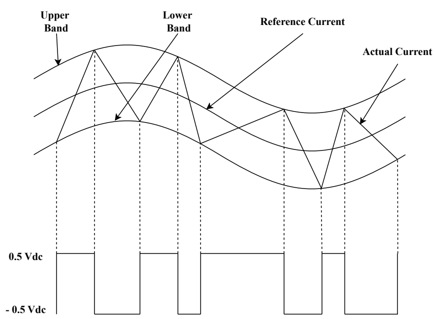

Figure 4: Hysterisis current controller with PWM pulses.

3. Result and Discussion

This Simulink model, shown in Figure 5, demonstrates the operation of a SAPF for harmonic reduction in a three-phase network with both balanced and unbalanced nonlinear loads. The process begins with the measurement of source voltage and load current, which are transformed into α-β-0 components using the Clarke transformation. These signals are then processed in the PQ Theory block to separate active and reactive power. A second-order filter extracts the AC part of active power, which, together with the PQ Theory, generates the reference currents in the α-β frame. The inverse Clarke transformation converts these reference currents back to the abc frame. A hysteresis current controller compares the reference and actual compensating currents to produce switching signals for the inverter. The inverter, connected via coupling inductors, injects harmonic compensating currents into the system. As a result, nonlinear load distortions are effectively suppressed, ensuring sinusoidal, balanced source currents with significantly reduced THD and enhanced power quality.

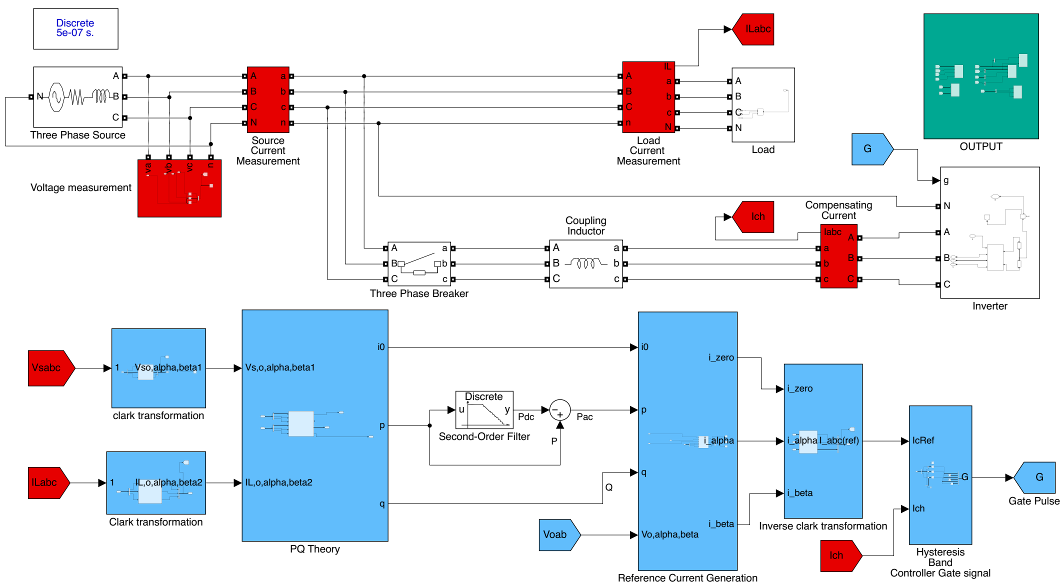

Figure 5: Simulink-based model representing the proposed SAPF.

3.1. Balanced Three-phase Non-linear Load

The simulation outcomes, demonstrated in Figure 6, show how an active compensator enhances power quality in a three-phase supply under nonlinear balanced load conditions, with detailed values provided in Table 2. In Figure 6, the first graph shows the source voltages that remain balanced and sinusoidal with an amplitude of about ±325 V. Initially, the source currents are distorted and the same as the load current before compensation up to 0.1sec and contain harmonic components due to the nonlinear load. However, after 0.1sec applying compensation, the source currents become nearly sinusoidal with magnitudes around ±14 A, reflecting a significant reduction in THD. The nonlinear load currents, shown in the third graph, are highly distorted and reach values up to ±12.35A as a result of harmonics generated by power electronic devices. To address this, the SAPF produces compensating currents of equal magnitude but having a phase shift of 180 degrees relative to harmonics, as illustrated in the fourth graph. Consequently, the SAPF maintains sinusoidal, balanced source currents, thereby reducing THD to below 0.29%, enhancing power quality, and ensuring efficient power utilization.

Figure 7 represents the Fourier analysis of the load current of balanced non-linear loads with detailed values provided in Table 2, showing that THD of 41.36%, which is relatively high. The harmonics spectrum indicates the presence of significant odd harmonics such as the 3rd, 5th, 7th, 9th, and higher orders. Odd harmonics are common in non-linear loads such as rectifiers, inverters, and other power electronic devices, and severely affect power quality.

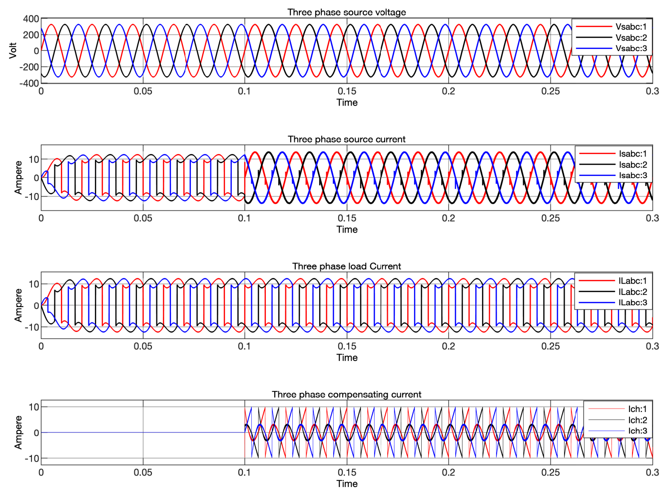

Figure 6: Simulation response for working of the SAPF for balanced three-phase non-linear load. (a) depicts the source voltage v_s; (b) depicts the source current i_s; (c) depicts the load current i_l; and (d) depicts the compensating current i_f.

In Figures 8, 9, and 10, it is observed that after applying the SAPF, the source currents are close to sinusoidal, with the THD for each phase reduced from 41.36% (uncompensated) to 0.25%, 0.28%, and 0.29%, respectively. The dominant odd harmonics, such as the 3rd, 5th, and 7th, are effectively mitigated, and only small residual components are visible, mainly around the higher orders, likely due to switching effects or

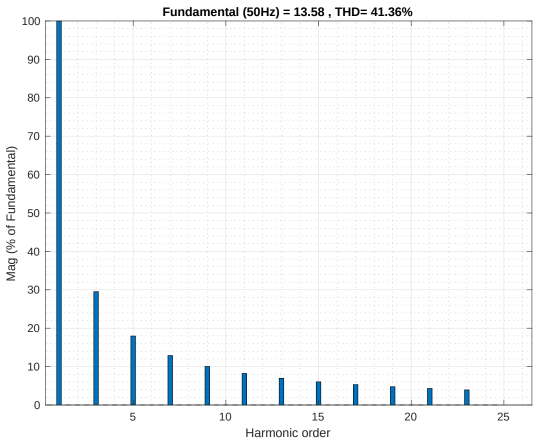

Figure 7: Harmonics spectrum of load current for non-linear balanced load.

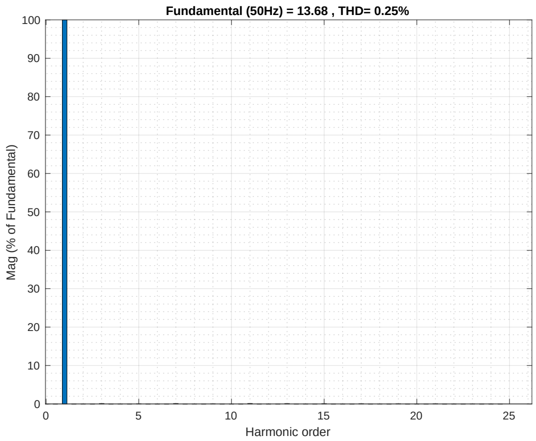

Figure 8: Phase A source current harmonics profile under non-linear balanced load.

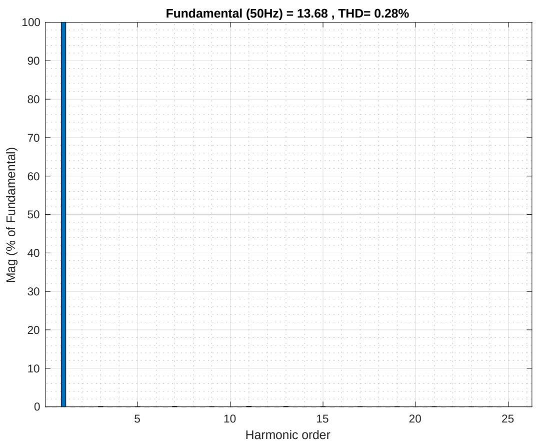

Figure 9: Phase B source current harmonics profile under non-linear balanced load.

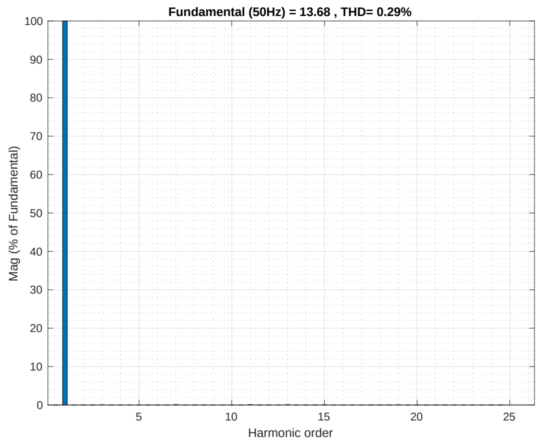

Figure 10: Phase C source current harmonics profile under non-linear balanced load.

minor compensation limitations. These results clearly demonstrate that the SAPF injects compensating currents, thereby suppressing harmonics and restoring the power factor close to unity.

3.2. Unbalanced Three-phase Non-linear Load

Table 1: Operating parameters

Electrical parameters	Value
AC voltage source	325 V_p
Frequency	50 Hz
Source impedance	R_S = 0.1 Ω, L_S = 10 mH
Coupling inductor	L_S = 0.5 mH
DC-link voltage	800 V

Table 2: Non-linear loads

Loads	R(□)	L(mH)
Non linear Balanced load	20	0.1
Non linear Unbalanced load		
R-Phase	40	0.8
Y-Phase	20	0.5
B-Phase	30	0.4

This Figure 11 shows the response of a three-phase system with a SAPF under unbalanced nonlinear load conditions with detailed values provided in Table 2. The first subplot presents balanced sinusoidal source voltages of about ±325 V. The second subplot shows source currents, initially distorted and unbalanced upto 0.1sec, source current becoming nearly sinusoidal after 0.1sec using SAPF compensation with magnitudes around ±10A. The third

Table 3: THDs of source current

No.	Load Specifications	% THD Source Current
I	Nonlinear Balanced system load without SAPF	41.36%
II	Nonlinear Balanced system load with SAPF	0.29%
III	Nonlinear Unbalanced system load without SAPF	46.05%
IV	Nonlinear Unbalanced system load with SAPF	1.81%

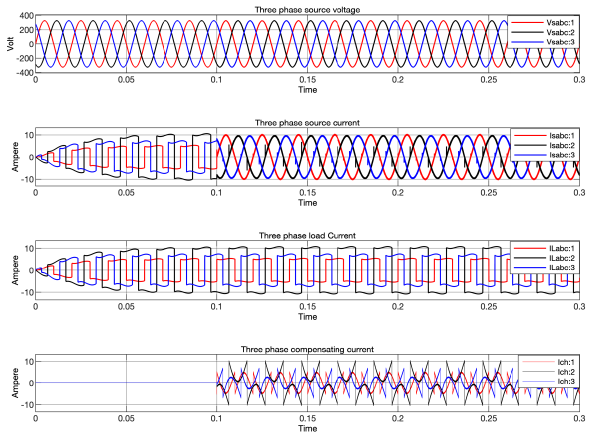

Figure 11: Simulation results for operation of the SAPF for unbalanced three-phase non-linear load. (a) depicts the source voltage v_s; (b) represents the source current i_s; (c) represents the load current i_l; and (d) represents the compensating current i_f.

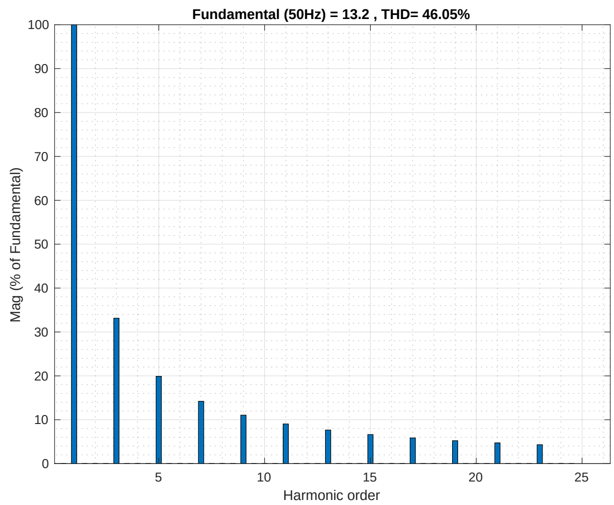

Figure 12: Harmonics spectrum of load current for unbalanced non-linear load.

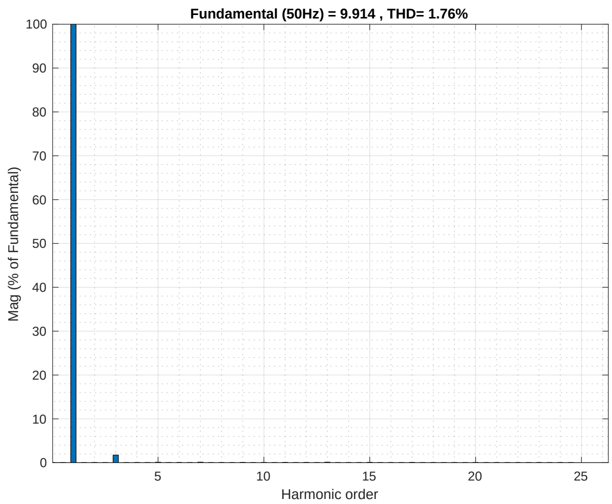

Figure 13: Phase A source current harmonics profile under non-linear unbalanced load.

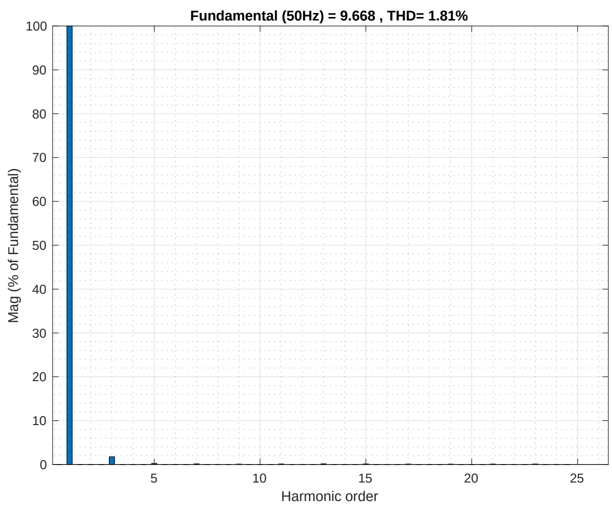

Figure 14: Phase B source current harmonics profile under non-linear unbalanced load.

subplot illustrates distorted and unbalanced load currents reaching up to ±10.75 A due to nonlinear devices. The fourth subplot depicts compensating currents injected by the SAPF, opposite to the harmonics, effectively canceling distortions and reducing THD to nearly 1.81%, thus improving power quality.

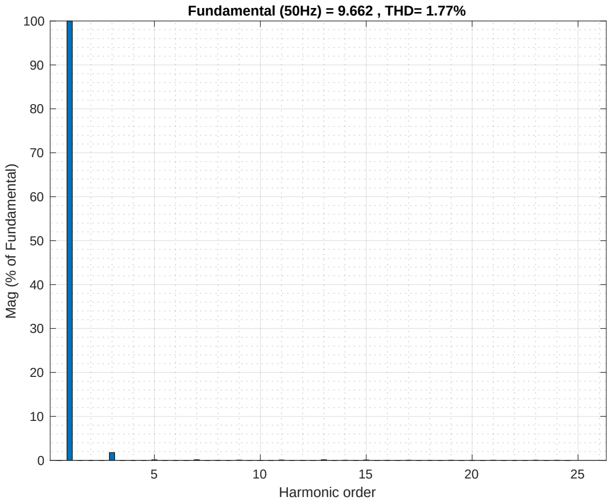

Figure 15: Phase C source current harmonics profile under non-linear unbalanced load.

Figure 12 presents the harmonic spectrum of the load current for an unbalanced nonlinear load. The fundamental component at 50 Hz has an amplitude of 13.2, while the THD reaches 46.05%, reflecting a significant waveform distortion. The spectrum is dominated by odd harmonics such as the third, fifth, seventh, and ninth, with magnitudes ranging from almost 30 to 35% of the fundamental value. These harmonics are primarily generated by nonlinear power electronic equipment combined with the effects of load unbalance, leading to considerable degradation in power quality.

The Figure 13, 14, and 15 present the harmonic spectrum of the source current after SAPF operation for an unbalanced nonlinear load. The 50 Hz fundamental remains dominant with an amplitude of about 9.91, while the THD decreases to 1.76%, 1.81%, and 1.77%, respectively, indicating a substantial reduction from the uncompensated case of 46.05%. Major odd harmonics such as the third, fifth, seventh, and ninth are significantly suppressed, leaving only minor residual components. Even harmonics, usually linked to load imbalance, appear at very low levels. Overall, the SAPF effectively mitigates harmonic content, producing nearly sinusoidal and balanced source currents, thereby enhancing power quality.

4. Conclusion

This work presents the design and simulation of a four-wire three-phase SAPF, developed using the IRPT concept and a hysteresis control algorithm in MATLAB/Simulink. The filter's performance in mitigating current harmonics is evaluated under different conditions, such as balanced and unbalanced nonlinear loads. Results confirm that the proposed filter effectively restores distorted source currents to nearly sinusoidal waveforms. Furthermore, it achieves harmonic reduction within the IEEE standard limits in all operating scenarios.

5. Limitation and Future Works

In the current study, nonlinear loads are represented as diode rectifiers with RL loads for both balanced and unbalanced system configurations under steady-state conditions. Further studies can incorporate more practical operating scenarios, involving time-varying balanced loads and varying nonlinear loads, to assess the dynamic performance and stability of the proposed SAPF control approach. Also, current control methods, such as PI-PWM, parabolic, ramp-time, dead-beat, MPC, and intelligent controllers (ANN/Fuzzy), can be used in the future to improve SAPF system dynamic response, eliminate harmonics, and improve overall efficiency. Additionally, a fixed DC voltage source is implemented rather than an actively regulated DC-link. Future research can implement a DC-link control loop employing a traditional PI controller or optimized control techniques such as GA, PSO, ANN, and MPC to maintain a stable DC-link voltage.

References

Adam, G., Stan, A. G., & Livinț, G. (2012). An adaptive hysteresis band current control for three phase shunt active power filter u sing fuzzy logic. *2012 International Conference and Exposition on Electrical and Power Engineering*, 324–329.

Adel, M., Zaid, S., & Mahgoub, O. (2011). Improved active power filter performance based on an indirect current control technique. *Journal of power electronics*, *11*(6), 931–937.

Afonso, J. L., Couto, C., & Martins, J. S. (2000). Active filters with control based on the pq theory.

Akagi, H., Kanazawa, Y., Fujita, K., & Nabae, A. (1983). Generalized theory of the instantaneous reactive power and its application. *The transactions of the Institute of Electrical Engineers of Japan. B*, *103*(7), 483–490.

Chang, G. W., & Shee, T.-C. (2004). A novel reference compensation current strategy for shunt active power filter control. *IEEE Transactions on Power Delivery*, *19*(4), 1751–1758.

Chavali, R. V., Dey, A., & Das, B. (2024). A performance comparison of hysteresis current control techniques for d-statcom application. *Electric Power Systems Research*, *234*, 110519.

Daniyal, H., Lam, E., Borle, L. J., & Iu, H. H. (2011). Hysteresis, pi and ramptime current control techniques for apf: An experimental comparison. *2011 6th IEEE Conference on Industrial Electronics and Applications*, 2151–2156.

F II, I. (1993). IEEE recommended practices and requirements for harmonic control in electrical power systems. *New York, NY, USA*, 1–1.

Hoon, Y., Mohd Radzi, M. A., Mohd Zainuri, M. A. A., & Zawawi, M. A. M. (2019). Shunt active power filter: A review on phase synchronization control techniques. *Electronics*, *8*(7), 791.

Imam, A. A., Sreerama Kumar, R., & Al-Turki, Y. A. (2020). Modeling and simulation of a pi controlled shunt active power filter for power quality enhancement based on pq theory. *Electronics*, *9*(4), 637.

Iqbal, M., Jawad, M., Jaffery, M. H., Akhtar, S., Rafiq, M. N., Qureshi, M. B., Ansari, A. R., & Nawaz, R. (2021). Neural networks based shunt hybrid active power filter for harmonic elimination. *IEEE Access*, *9*, 69913–69925.

Kanagavel, R., & Indragandhi, V. (2019). Current control techniques of single phase shunt active power filter-a review. *IOP conference series: materials science and engineering*, *623*(1), 012007.

Kanjiya, P., Khadkikar, V., & Zeineldin, H. H. (2012). A noniterative optimized algorithm for shunt active power filter under distorted and unbalanced supply voltages. *IEEE Transactions on Industrial Electronics*, *60*(12), 5376–5390.

Kmail, M. (2012). Investigation of shunt active power filter for power quality improvement. *NEAR EAST*.

Mikkili, S., & Panda, A. K. (2011a). Shaf for mitigation of current harmonics using pq method with pi and fuzzy controllers. *Engineering, Technology & Applied Science Research*, *1*(4), 98–104.

Mikkili, S., & Panda, A. K. (2011b). Simulation and rtds hardware implementation of shaf for mitigation of current harmonics with pq and id-iq control strategies using pi controller. *Engineering, Technology & Applied Science Research*, *1*(3), 54–62.

Sahu, G., Patjoshi, R. K., & Panigrahi, R. (2020). An fpga based novel digital controller for dstatcom to enhance power quality in distribution system. *ECTI Transactions on Electrical Engineering, Electronics, and Communications*, *18*(2), 118–129.

This page is intentionally left blank.